Six-photon entangled Dicke state enabled by a UV enhancement cavity as novel SPDC photon source

Witlef Wieczorek[a,b], Roland Krischek[a,b], Akira Ozawa[a], Géza Tóth[c,d,e], Nikolai Kiesel[a,b], Patrick Michelberger[a,b], Thomas Udem[a], Harald Weinfurter [a,b]

[a]Max-Planck-Institut für Quantenoptik, Hans-Kopfermann-Strasse 1, D-85748 Garching, Germany;
[b] Fakultät für Physik, Ludwig-Maximilians-Universität, D-80797 München, Germany;
[c]Department of Theoretical Physics, The University of the Basque Country, PO Box 644, E-48080 Bilbao, Spain;
[d]IKERBASQUE, Basque Foundation for Science, Alameda Urquijo 36, E-48011 Bilbao, Spain;
[e]Research Institute for Solid State Physics and Optics, Hungarian Academy of Sciences, PO Box 49, H-1525 Budapest, Hungary

ABSTRACT

Photon sources for multi-photon entanglement experiments are commonly based on the process of spontaneous parametric down conversion. Due to the probabilistic photon production, such experiments suffer from low multi-photon count rates. To increase this count rate, we present a novel SPDC pump source based on a femtosecond UV enhancement cavity that increases the available pump power while maintaining a high repetition rate of 80 MHz. We apply the cavity as photon source for realizing symmetric, multi-partite entangled Dicke states, which are observed with a high rate and high fidelity. We characterize the observed Dicke states of up to six photons using efficient tools exploiting the state's symmetries.

Keywords: quantum optics, quantum information, multi-photon entanglement, non-classical states, nonlinear optics, optical resonators

1. INTRODUCTION

Multi-partite entanglement plays a decisive role in most quantum information tasks. Thus, the experimental realization of entanglement is crucial for progressing beyond classical information processing. For this purpose, photons are a preferred physical system as they can be easily transmitted, controlled and well decoupled from the environment.[1–3] Experimental setups for photonic quantum information processing commonly use a photon source based on the process of spontaneous parametric down conversion (SPDC) and linear optical elements together with conditional detection. This approach has been successfully applied for proof-of-principle demonstrations of quantum information applications[4–12] and for observations of multi-partite entangled states.[13–25]

In particular, for multi-photon experiments, the count rate of higher photon number states drastically decreases due to the probabilistic photon production in the SPDC process. Therefore, it is a common approach to concentrate the required pump power in trains of intense ultrashort pulses. This significantly increases the probability of simultaneous SPDC photon production events compared to cw-pump sources. Pulsed SPDC pump systems for multi-photon entanglement experiments mostly use ultraviolet (UV) pulses derived from frequency-doubled Ti:sapphire oscillators to obtain SPDC photons in the infrared (IR) wavelength range (~ 800 nm). SPDC photons at IR wavelengths are desired because high efficiency ($\sim 60\,\%$), single photon detectors (silicon avalanche

Send correspondence to W.W.: E-mail: witlef.wieczorek@mpq.mpg.de
Present address A.O.: Institute for Solid State Physics, University of Tokyo, Kashiwa, Chiba 277-8581, Japan
Present address N.K.: Quantum Optics, Quantum Nanophysics and Quantum Information, Faculty of Physics, University of Vienna, A-1090 Vienna, Austria
Present address P.M.: Clarendon Laboratory, University of Oxford, Oxford OX1 3PU, UK

Quantum Optics, edited by Victor N. Zadkov, Thomas Durt, Proc. of SPIE Vol. 7727, 77270L © 2010 SPIE · CCC code: 0277-786X/10/$18 · doi: 10.1117/12.853599

photo diodes) at this wavelength range are commercially available. However, count rates of six-photon experiments using commercially available laser systems are rather low (so far, typically, some events per hour[23,25]). Here, we describe a novel SPDC pump source,[26] which allows to perform high-rate multi-photon entanglement experiments. The photon source, described in Sec. 2, utilizes a femtosecond UV enhancement cavity, which drastically increases the available SPDC pump power to about 7 W at a repetition rate of 81MHz with a pulse width of about 180 fs centered around a wavelength of 390 nm.

Furthermore, we use the photon source in combination with a linear optical network for the experimental observation of symmetric Dicke states of up to six photons[24,25] (Sec. 3). The novel SPDC source allows the realization of these Dicke states with a high fidelity and high count rate. For the state analysis we apply efficient tools, which allow to prove entanglement and to estimate the fidelity without requiring a full reconstruction of the density matrix.[27]

2. PHOTON SOURCE: UV ENHANCEMENT CAVITY

2.1 Expected multi-photon count rate

Let us first estimate the expected count rate for multi-photon states. The N photon count rate c_ψ obtained in an experiment is determined first by the yield of the SPDC source, second by the linear optical network, if, upon conditional detection, only a fraction of the N photon emission leads to the desired state $|\psi\rangle$ and third, by the detection efficiency.[28] Let us consider a collinear type II SPDC process, which emits the state[29]

$$|\psi\rangle_{\mathrm{SPDC}} = \sqrt{1-\tanh^2\tau}\sum_{n=0}^{\infty}\tanh^n\tau\,|n_H, n_V\rangle \tag{1}$$

into a single spatial mode. Here, H (V) denotes horizontal (vertical) polarization and τ is the coupling parameter of the crystal with the electric field of the pump. This parameter is directly proportional to the pump field and the nonlinearity of the crystal.[29] For low pump powers, we can approximate $\tanh\tau \approx \tau$ and obtain the probability for an N-photon generation event as τ^N with $N = 2n$. The generation rate is then $\tau^N f_{\mathrm{rep}}$, whereby f_{rep} is the repetition rate of the pulsed pump laser. Further, the overall detection efficiency for N photons (η_{det}^N) and the probability of observing the state in the linear optical setup (p_ψ) contribute to the total rate of N detected photon events:

$$c_\psi = \tau^N f_{\mathrm{rep}} \eta_{\mathrm{det}}^N p_\psi. \tag{2}$$

Hence, high repetition rates, high efficiencies and high pump powers are required. Before we calculate the expected count rates, we consider different multi-partite entangled states and their observation probabilities. These vary as each state requires a dedicated linear optical setup. Focusing on well-known multi-partite quantum states, as for example the Greenberger-Horne-Zeilinger (GHZ) states $|\mathrm{GHZ}_N\rangle = (|H\rangle^{\otimes N} + |V\rangle^{\otimes N})/\sqrt{2}$[30] (with $|H\rangle^{\otimes N} = |H\ldots H\rangle_{1,\ldots,N}$), the singlet states $|\Psi_N^-\rangle$[31,32] and the Dicke states $|D_N^{(N/2)}\rangle$[33,34] (see eq. 6), we find for their particular linear optical realizations: $p_{\mathrm{GHZ}_N} = 2^{-(N/2-1)}$ (Refs.[13,14,30]), $p_{\Psi_N^-} = [(N/2)!/(N/2)^{N/2}]^2$ (Refs.[23,35]) and $p_{D_N^{(N/2)}} = N!/N^N$ (Refs.[19,24,25]).

As an example, let us apply eq. 2 to the observation of the Dicke state $|D_4^{(2)}\rangle$ reported in Ref.[19] By using a typical pump laser system (0.6 W, 81 MHz, 130 fs, 390 nm), the following parameters have been achieved (taken from Refs.[19,36]): $\tau^2 = 0.034$, $\eta_{\mathrm{det}} = 0.1$ and $p_{D_4^{(2)}} = 0.08$. This results in a total calculated rate $c_{D_4^{(2)}} = 0.75\,\mathrm{s}^{-1}$, which agrees quite well with the measured rate of $1\,\mathrm{s}^{-1}$. However, using the same pump source for observing the six-photon state $|D_6^{(3)}\rangle$ ($p_{D_6^{(3)}} = 0.0154$) would yield a rate of $c_{D_6^{(3)}} = 0.00005\,\mathrm{s}^{-1} = 0.18\,\mathrm{h}^{-1}$. This is far too low for acquiring sufficient statistics in a sensible measurement time.

In contrast, our novel approach as described in Sec. 2.2 results in values of up to $\tau = 0.46$ ($P_{\mathrm{UV}} = 7.2$ W) with an efficiency of $\eta_{\mathrm{det}} = 0.15$.[26] This yields for the state $|D_6^{(3)}\rangle$ a calculated count rate of 8 six-photon events per minute. This rate is suitable for performing an in-depth six-photon state characterization.[24] The next step for multi-photon experiments would be to realize eight-photon entangled states. Assuming $\tau = 0.5$ at a repetition rate of $f_{\mathrm{rep}} = 80$ MHz and an efficiency of $\eta_{\mathrm{det}} = 0.15$ yields $c_\psi = (4.8 \cdot p_\psi)\,\mathrm{min}^{-1}$. Using now the various

state probabilities p_ψ we find the following rates: $c_{\mathrm{GHZ}_8} = 0.6\,\mathrm{min}^{-1} = 36\,\mathrm{h}^{-1}$, $c_{\Psi_8^-} = 0.042\,\mathrm{min}^{-1} = 2.5\,\mathrm{h}^{-1}$ and $c_{D_8^{(4)}} = 0.011\,\mathrm{min}^{-1} = 0.69\,\mathrm{h}^{-1}$. With these numbers, the observation of the eight-photon GHZ state is in immediate experimental reach.

One has to keep in mind that an increase in pump power together with a less than unit detection efficiency and the absence of photon-number resolving detectors also increases the noise contribution originating from higher order SPDC emissions.[37,38] Hence, pump powers must not be too high either. This excludes the utilization of Ti:sapphire amplifier systems,[39] which actively amplify IR pulses on the cost of a drastically reduced repetition rate. Other Ti:sapphire laser designs to increase the pump power usually on the cost of a reduced repetition rate (like chirped pulse Ti:sapphire oscillators[40]) are described for example in Ref.[41] Therefore, our approach maintains the repetition rate of the driving laser and at the same time increases the UV pump power by using a passive enhancement cavity.

We would like to note that high efficiency detectors would strongly reduce noise and increase the count rate. However, to date, commercially available silicon avalanche photo diodes are still the best detectors for the IR wavelength range offering efficiencies with up to 60%, whereby future improvement can be expected from superconducting detectors.[42–44]

2.2 Design criteria of the cavity

Enhancement cavities for the femtosecond regime have been demonstrated in the IR wavelength region, where they have been used for second harmonic generation[45] and high harmonic generation.[46–48] Resonant cavity enhancement is exactly achieved for a cw-laser, since it is described by a single frequency mode. It can also be achieved for a mode-locked train of ultrashort pulses whose frequency spectrum is composed of a frequency comb,[49] which can be written as

$$\omega_n = n\omega_{\mathrm{rep}} + \omega_{\mathrm{ceo}}, \tag{3}$$

with $\omega_{\mathrm{rep}} = 2\pi f_{\mathrm{rep}}$, n the mode number and ω_{ceo} the carrier envelope offset frequency. Thus, to enhance a train of ultrashort pulses in a cavity, all the frequencies of the comb have to be resonant with the cavity modes, which requires that

- the cavity round trip time has to match the inverse of the repetition rate of the laser pulses,
- ω_{ceo} is appropriately set, such that the frequency comb of the laser pulses match the cavity resonances, and
- the pulse shape inside the cavity has to be preserved, which means that dispersion is minimized.

The first two conditions can be fulfilled by adjusting experimental parameters, as described below. The third requirement is linked to the influence of frequency-dependent phase shifts, i.e., dispersion, which displace certain cavity resonances with respect to the frequency modes of the external laser pulses, such that resonant enhancement is diminished. To compensate the dispersion introduced, e.g., by air or other dispersive media, the cavity has to be redesigned, for example, by using chirped mirrors[50] or evacuating the cavity.

The expected frequency-dependent power enhancement $P_{\mathrm{E}}(\omega)$ achievable with dispersion and loss in the cavity can be calculated from[51,52]

$$P_{\mathrm{E}}(\omega) = \frac{|t_{\mathrm{IC}}(\omega)|^2}{1 + |r(\omega)|^2 - 2|r(\omega)|\cos\phi(\omega)}, \tag{4}$$

whereby $t_{\mathrm{IC}}(\omega)$ is the frequency-dependent transmittivity for the laser electric field at the input coupler (IC), $r(\omega) = r_{\mathrm{IC}}(\omega) r_{\mathrm{cav}}(\omega)$ is the overall reflectivity of the cavity (including all mirrors and other loss channels) and $\phi(\omega)$ is the phase shift collected after one round trip. Assuming a certain intrinsic loss $1 - |r_{\mathrm{cav}}|^2$ inside the cavity, the impedance matching condition ($|t_{\mathrm{IC}}(\omega)|^2 = 1 - |r_{\mathrm{cav}}|^2$) has to be fulfilled in order to achieve maximal power enhancement of $P_{\mathrm{E,max}} = 1/|t_{\mathrm{IC}}(\omega)|^2$ for $\phi(\omega) = 0$. Dispersion results in a non-zero and frequency-dependent phase shift $\phi(\omega)$, which can be expanded in a Taylor series around a particular frequency ω_0

$$\phi(\omega) = \phi(\omega_0) + \phi'(\omega_0)(\omega - \omega_0) + \Delta\phi(\omega). \tag{5}$$

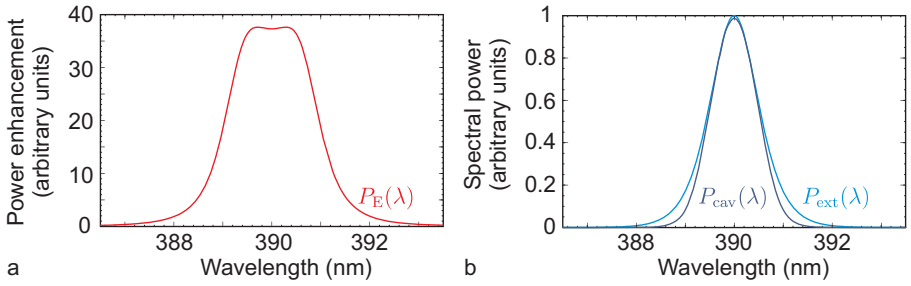

Figure 1. (a) Calculated power enhancement for the UV enhancement cavity including intra-cavity dispersion and 2.66% loss. (b) External (P_{ext}) and intra-cavity spectrum (P_{cav}) for the scenario of (a).

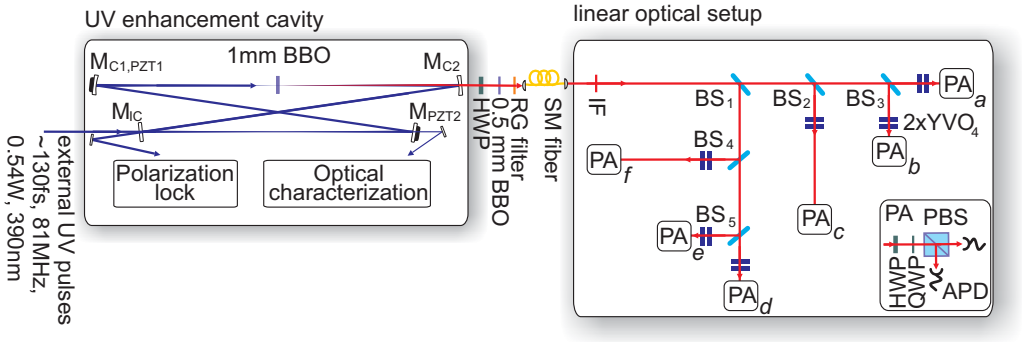

Figure 2. The four mirrors (M_{IC}, input coupler; $M_{C1,PZT1}$, curved mirror on piezoelectric transducer; M_{C2}, curved and dichroic mirror; M_{PZT2}, mirror on piezoelectric transducer) make up the UV enhancement cavity. The linear optical setup is used to observe multi-photon entangled Dicke states $|D_N^{(N/2)}\rangle$ with $N \leq 6$ and even N. Further details see main text.

Here $\Delta\phi(\omega)$ includes group delay dispersion (GDD) and higher order effects, which distort the cavity frequency comb from being equidistant.[52] For our case, the major contributions originate from air (190 fs^2 GDD) and the 1 mm thick non-linear crystal (190 fs^2 GDD), while the dispersion introduced by the mirrors can be neglected.

Fig. 1(a) shows the calculated frequency-dependent power enhancement for a total expected loss of 2.66% originating from the non-linear crystal, air and the mirrors. Theoretically, this would yield a maximal power enhancement of 38 when neglecting dispersion. When including dispersion a frequency-averaged power enhancement of 33 can be achieved. Fig. 1(b) shows the corresponding intra-cavity spectrum, when a sech-shaped spectrum with a full-width at half maximum of 1.15 nm is used as input to the cavity. The external and intra-cavity spectrum are scaled such that they touch at the points of zero dispersion. Away from zero dispersion the enhancement is slightly diminished, most pronounced in the wings of the intra-cavity spectrum. Improvements could be made by selecting chirped mirrors,[50] which compensate for this effect.

2.3 Experimental implementation and results

In the experiment, the enhancement cavity is implemented in a four-mirror, bow tie shape (Fig. 2). Its length is determined by the temporal separation of the pulses (1/81 MHz = 12 ns) and amounts to ~ 3.7 m. The input coupling mirror has a transmission of 2.5% at 390 nm, which approximately fulfills the impedance matching condition to compensate for the expected loss inside the cavity. The other three mirrors are highly reflective for 390 nm (better than 99.98% reflectivity), of which two mirrors are curved (radius of curvature -800 mm) to obtain two intra-cavity beam waists (100 μm and 330 μm). One of the curved mirrors is a dichroic mirror, which transmits light at 780 nm corresponding to the wavelength of the SPDC photons generated by the non-linear crystal [β barium borate (BBO)] placed at the smaller waist. While the intra-cavity mode is closely represented by a TEM_{00} beam ($M^2 = 1.15 \pm 0.03$), the external laser beam has an elliptical profile. A set of cylindrical lenses is used to approximately mode match the external to the intra-cavity transversal mode profile. Moreover, the

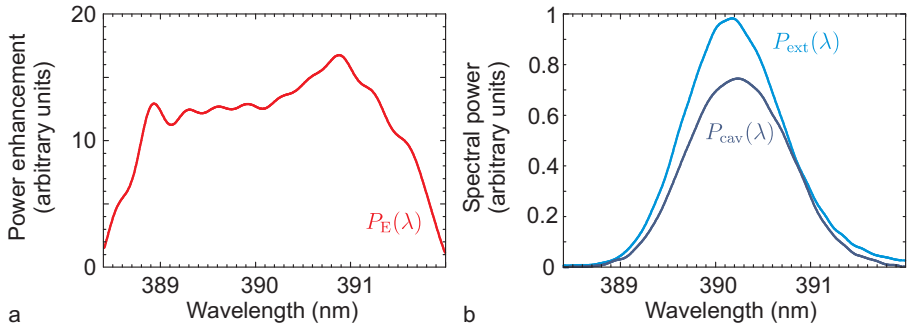

Figure 3. (a) Experimentally obtained power enhancement for the UV enhancement cavity derived from the measured (b) external (P_{ext}) and intra-cavity spectrum (P_{cav}).

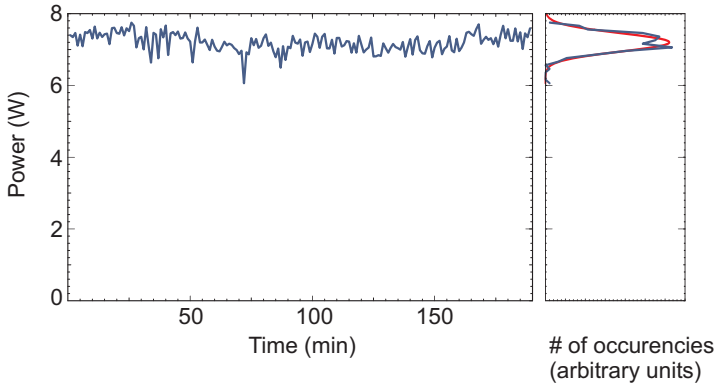

Figure 4. Intra-cavity power over more than three hours of stable locking. A histogram of the power level shows near Gaussian-like distribution (red) with (7.2 ± 0.26) W.

laser beam is actively stabilized in position and direction to compensate beam fluctuations originating from the Ti:sapphire oscillator or the second harmonic generation unit.

To enhance the external laser pulses in the cavity, both degrees of freedom (ω_{rep} and ω_{ceo}) of the external and intra-cavity frequency combs, respectively, have to match. To this end, the cavity length is actively adjusted via piezoelectric transducers, which are controlled by a polarization lock[53,54] to yield a free spectral range resembling the repetition rate of the laser pulses (ω_{rep}). The polarization lock is fed by a spectrally selected feedback signal in order to set the intra-cavity center wavelength. The offset frequency ω_{ceo} of the laser pulses can either be adjusted by varying the dispersion inside the Ti:sapphire oscillator via prism insertion or by changing the pump power of the Ti:sapphire oscillator,[55] whereby the former possibility has been chosen. This results, in our case, in a stability of ω_{ceo} of hours. Hence, it only has to be adjusted once for optimal power, while during the experiment, a software-controlled loop optimizes occasionally the prism insertion of the Ti:sapphire oscillator for achieving maximal intra-cavity power.

With this configuration we achieve up to 7.2 W optical power inside the cavity, which corresponds to a 13.3 times enhancement of the external laser pulses of 0.54 W. Even though external laser pulses with a higher average power would be available, the achieved UV intra-cavity power is still greater than a factor of five compared to what can be obtained from commercially available, high power, frequency-doubled Ti:sapphire oscillator systems (1.4 W UV, 80 MHz, 200 fs, 400 nm). Hence, by using such systems, our achieved power enhancement of 13.3 could result in intra-cavity UV powers of more than 18 W, if the non-linear crystal is not damaged.

The spectrally-resolved power enhancement and the intra-cavity spectrum are shown in Fig. 3 (compare to theoretical calculations shown in Fig. 1). The power enhancement has a near flat spectral dependence over the relevant wavelength region without pronounced spikes or dips. However, the intra-cavity spectrum does not perfectly resemble the external spectrum, which can be attributed to dispersion inside the cavity stemming

from air and the non-linear crystal. The discrepancy between the achieved power enhancement of 13.3 and the calculated value of 33 can be mainly attributed to the non-perfect mode-matching of the external to the intra-cavity beam. Approximately 50 % of the external laser mode is coupled resonantly into the TEM_{00} cavity mode. Taking this into account, one would have a twice as high enhancement of roughly 25, which approaches the calculated value. Since, most importantly, long-term stability is required for multi-photon experiments, Fig. 4 shows the intra-cavity power during a run time of more than three hours. A nearly Gaussian-distributed power fluctuation of less than 4% is observed. This UV enhancement cavity can thus be used as pump source for the SPDC process, which is outlined in the following section.

3. EXPERIMENTAL OBSERVATION OF DICKE STATES

3.1 Dicke states

Dicke states[33,34] represent an important resource in quantum information. They are eigenstates of the squared total angular momentum $\hat{J}^2$ and its z component $\hat{J}_z$ ($\hat{J}_i = 1/2 \sum_l \hat{\sigma}_i^l$ with $\hat{\sigma}_i^l$ being the Pauli matrix $i \in \{x, y, z\}$ acting on the l^{th} qubit). We focus on the symmetric Dicke states $|\, D_N^{(e)} \,\rangle$ with $\hat{J}^2 \,|\, D_N^{(e)} \,\rangle = N/2(N/2+1)\,|\, D_N^{(e)} \,\rangle$ and $\hat{J}_z \,|\, D_N^{(e)} \,\rangle = (N/2 - e)\,|\, D_N^{(e)} \,\rangle$, where

$$|\, D_N^{(e)} \,\rangle = \left(\begin{array}{c} N \\ e \end{array} \right)^{-1/2} \sum_i \mathcal{P}_i \,|\, H^{\otimes(N-e)} V^{\otimes e} \,\rangle, \tag{6}$$

and $\mathcal{P}_i \,|\, H^{\otimes(N-e)} V^{\otimes e} \,\rangle$ denotes all distinct permutations of $|\, H^{\otimes(N-e)} V^{\otimes e} \,\rangle$ comprising e $(N - e)$ vertically (horizontally) polarized photons.

Initially, these states were studied in the context of enhanced light emission from a cloud of atoms.[33] In the meantime, Dicke states have also been found relevant for quantum information processing. They constitute a rich resource of inequivalent states of a lower qubit number obtained via projective measurements.[19,24,25,37] Thereby, state inequivalence can, for example, be classified according to the criterion of stochastic local operations and classical communication (SLOCC).[56,57] Further, it has also been shown that Dicke states, in particular the states $|\, D_N^{(1)} \,\rangle$ [56,58] (usually called W states) and $|\, D_N^{(N/2)} \,\rangle$,[19,24,25] are persistent against particle loss. That means, some entanglement remains in the states obtained after losing particles. In contrast, this is not the case for, e.g., $|\, \mathrm{GHZ}_N \,\rangle$ states, where a separable state is obtained after particle loss. Most importantly, Dicke states can also be used for quantum information applications like telecloning,[19,59] open-destination teleportation,[16,19] secret sharing[19,25,60] and quantum metrology.[24,61,62] Finally, Dicke states have appeared in the context of classifications of quantum states. For example, using the SLOCC-classification criterion two different classes of genuine tri-partite entanglement have been discovered: the GHZ class and the W (Dicke state $|\, D_3^{(1)} \,\rangle$) class. Recently, a classification of all symmetric states has been carried out,[63] whereby Dicke states appear naturally.

3.2 Experimental observation

For our experiment (Fig. 2) we use the collinear type II SPDC emission (eq. 1), which delivers in its n^{th} order the state $|\, n_H, n_V \,\rangle$. Subsequent distribution of these photons into $N = 2n$ spatial modes leads to the observation of the states $|\, D_N^{(N/2)} \,\rangle$ conditioned upon coincident single photon detection in each spatial mode. This occurs with the finite probability of $p_{D_N^{(N/2)}} = N!/N^N$. Generally, symmetrization of N photons in particular polarization states initially located in a single spatial mode into N spatial modes leads to superpositions of Dicke states. This has been recently described in Ref.[64] with respect to the observation of all symmetric photonic states.

In the experiment, the photons of the collinear type II SPDC emission from the BBO crystal inside the cavity have to be indistinguishable in all degrees of freedom except for the polarization degree. To guarantee spatial indistinguishability of the SPDC photons, they are coupled into a single mode fiber[65] (SM). Walk-off effects caused in the BBO crystal and the resulting temporal distinguishability between H and V polarized photons is compensated with a half-wave plate (HWP) together with a 0.5 mm thick BBO crystal placed in the SPDC beam.[66] A 3 nm FWHM interference filter (IF), centered around 780 nm, spectrally selects the SPDC photons.[67,68]

Polarization-independent beam splitter cubes (BS) symmetrically distribute the SPDC photons into the six spatial modes a, b, c, d, e, f, see Fig. 2. Due to non-ideal splitting ratios of the BSs the observation probability for the state $|D_6^{(3)}\rangle$ reduces by 20% from 0.0154 to 0.0126. Birefringence caused by the dielectric coating of the beam splitters is compensated for by employing two perpendicularly oriented, 200 μm thick yttrium-vanadate crystals (YVO_4) in each mode. Finally, state analysis is performed using a half- and a quarter-wave plate (QWP) in front of a polarizing beam splitter cube (PBS). This allows us to measure all possible standard bases ($\hat{\sigma}_x$, $\hat{\sigma}_y$, $\hat{\sigma}_z$) on each qubit, thereby characterizing the experimentally realized states. The photons are detected with silicon-avalanche photo diodes (APD), whose detection signals are fed into a field programmable gate array (FPGA) controlled coincidence logic.[28] The FPGA logic is synchronously clocked by the repetition rate of the Ti:sapphire laser and allows us to simultaneously register all possible coincidences between the 12 detectors.

The experimental setup also allows for the observation of the states $|D_4^{(2)}\rangle$ or $|D_2^{(1)}\rangle$ when selecting only coincidences in four (e.g. a, b, c, d) or two spatial modes (e.g. a, b), respectively. This conditions the detection ideally on the 2nd or 1st order SPDC emission, respectively.

For the measurement, we use a UV pump power of 5.3 W, which is lower than the maximally possible intra-cavity power. We chose that pump power to guarantee long-term stability of the cavity (on the order of > 20 h) and at the same time reduce the influence of noise originating from higher order SPDC events.[37,38] We achieve a six-photon count rate of 3.6 min^{-1}, which is more than an order of magnitude higher than count rates of comparable multi-photon experiments.[23,25] We would like to note that the UV enhancement cavity allows to tune the available UV pump power over a wide regime: achieving high fidelity states on the cost of low count rates for low pump powers up to high count rates achieved with high pump powers, but sacrificing state fidelity.

3.3 Characterization

Efficient tools have been introduced to characterize the entanglement of Dicke states.[27,69,70] Here, we focus on proving genuine N-partite entanglement[71] and estimating the fidelity with a few measurement settings. Entanglement witnesses are an ideal tool to detect entanglement.[72] For the states $|D_N^{(N/2)}\rangle$, the generic witness operators[69,73]

$$\hat{\mathcal{W}} = \frac{N}{2(N-1)}\mathbb{1}^{\otimes N} - |D_N^{(N/2)}\rangle\langle D_N^{(N/2)}| \tag{7}$$

have been constructed. A negative expectation value signals genuine N-partite entanglement as the value $N/[2(N-1)]$ is the maximal overlap of the state $|D_N^{(N/2)}\rangle$ with any bi-separable state. Yet, these witness operators require the determination of the fidelity $F = \mathrm{Tr}(\rho\,|D_N^{(N/2)}\rangle\langle D_N^{(N/2)}|)$ of the experimentally measured state ρ to the ideal Dicke state $|D_N^{(N/2)}\rangle$. To this end, an increasing number of measurement settings in the standard bases ($\hat{\sigma}_x$, $\hat{\sigma}_y$, $\hat{\sigma}_z$) with higher N is required (for $N = 4$: 21, $N = 6$: 183). Changing to rotated basis settings reduces the effort drastically (for $N = 4$: 9, $N = 6$: 21).[27,70]

However, more efficient witnesses exist, which exploit the definition of Dicke states via the angular momentum operators:

$$\hat{\mathcal{W}}' = \alpha_{\mathrm{bi-sep},N} \cdot \mathbb{1}^{\otimes N} - \left(\hat{J}_x^2 + \hat{J}_y^2\right), \tag{8}$$

whereby $\alpha_{\mathrm{bi-sep,N}}$ denotes the maximal overlap of the states $|D_N^{(N/2)}\rangle$ with any bi-separable state (see Table 1). Experimentally, the expectation value $\langle\hat{\mathcal{W}}'\rangle$ can be determined from a measurement of all qubits along the $\hat{\sigma}_x$ and $\hat{\sigma}_y$ direction. We obtain the values given in Table 1, which clearly demonstrate genuine N-partite entanglement.

It is also possible to estimate the fidelity with only a few measurements, as efficient witnesses $\hat{\mathcal{W}}''$ can be constructed, which are based on the generic witness (eq. 7). They have to fulfill the condition $\hat{\mathcal{W}}'' - \xi\hat{\mathcal{W}} \geq 0$ for some $\xi > 0$.[27] This condition means that the expectation value with any bi-separable state remains positive. Using the angular momentum operators, such witnesses can be written as[27]

$$\hat{\mathcal{W}}'' = c_0\mathbb{1}^{\otimes N} + \sum_{l\in\{x,y,z\}}\sum_{n=1}^{N} c_{ln}(\hat{J}_l)^n, \tag{9}$$

whereby c_0, c_{ln} can be determined numerically.[27] As only the operators $\hat{J}_x$, $\hat{J}_y$ and $\hat{J}_z$ and their powers occur in this formula, the three measurement settings $\hat{\sigma}_x$, $\hat{\sigma}_y$ and $\hat{\sigma}_z$ on each qubit are sufficient for evaluating $\hat{\mathcal{W}}''$. A lower bound on the fidelity F^{lb} can then be estimated via[27]

$$F \geq F^{\mathrm{lb}} = \frac{N}{2(N-1)} - \langle \hat{\mathcal{W}}'' \rangle / \xi. \tag{10}$$

Experimentally, we obtain the fidelities given in Table 1. These values are also sufficient to prove N-partite entanglement by establishing a lower bound on the expectation value of the generic witness (eq. 7 and Table 1).

The utilized witnesses can also be applied to states derived from $|\, D_N^{(N/2)} \,\rangle$ by projective measurements or qubit loss. This is described in detail in Refs.[24, 27, 37]

Table 1. Experimental results for proving genuine N-partite entanglement using witness operators $\hat{\mathcal{W}}'$ and for estimating the fidelity F^{lb}.

state	$\alpha_{\mathrm{bi-sep,N}}$	$\langle \hat{\mathcal{W}}' \rangle$	F^{lb}
$\|\, D_4^{(2)} \,\rangle$	5.232	-0.373 ± 0.008	0.76 ± 0.001
$\|\, D_6^{(3)} \,\rangle$	11.0179	-0.422 ± 0.148	0.64 ± 0.016

4. SUMMARY

We have designed and characterized a novel UV enhancement cavity for femtosecond pulses. The cavity enhances the average UV power of the incoming pulses by more than a factor of 13 in spite of dispersion of air and a non-linear crystal. More than 7 W UV power at 81 MHz repetition rate with sub 200 fs pulse duration are available to drive non-linear processes. In the future, even stronger enhancement can be achieved by the use of chirped mirrors that are tailored to the cavity dispersion.

We have applied the cavity to drive the non-linear process of spontaneous parametric down conversion. The high pump power increases the multi-photon yield in SPDC drastically. We have designed a linear optical network that symmetrically distributes the SPDC photons to observe the states $|\, D_N^{(N/2)} \,\rangle$ with $N \leq 6$. Efficient tools have allowed us to prove their entanglement and to estimate their fidelity.

ACKNOWLEDGMENTS

We acknowledge the support of this work by the DFG-Cluster of Excellence MAP, the EU Projects QAP and Q-Essence, and the DAAD/MNiSW exchange program. W.W. acknowledges support by QCCC of the Elite Network of Bavaria.

REFERENCES

1. J. L. O'Brien, "Optical quantum computing," *Science* **318**(5856), pp. 1567–1570, 2007.
2. J.-W. Pan, Z.-B. Chen, M. Zukowski, H. Weinfurter, and A. Zeilinger, "Multi-photon entanglement and interferometry," *arXiv: 0805.2853 [quant-ph]* , 2008.
3. J. L. O'Brien, A. Furusawa, and J. Vuckovic, "Photonic quantum technologies," *Nat. Photon.* **3**, pp. 687–695, Dec. 2009.
4. D. Bouwmeester, J.-W. Pan, K. Mattle, M. Eibl, H. Weinfurter, and A. Zeilinger, "Experimental quantum teleportation," *Nature* **390**, pp. 575–579, Dec. 1997.
5. J.-W. Pan, D. Bouwmeester, H. Weinfurter, and A. Zeilinger, "Experimental entanglement swapping: Entangling photons that never interacted," *Phys. Rev. Lett.* **80**(18), pp. 3891–3894, 1998.
6. P. Walther, K. J. Resch, T. Rudolph, E. Schenck, H. Weinfurter, V. Vedral, M. Aspelmeyer, and A. Zeilinger, "Experimental one-way quantum computing," *Nature* **434**, pp. 169–176, Mar. 2005.

7. B. P. Lanyon, T. J. Weinhold, N. K. Langford, M. Barbieri, D. F. V. James, A. Gilchrist, and A. G. White, "Experimental demonstration of a compiled version of shor's algorithm with quantum entanglement," *Phys. Rev. Lett.* **99**(25), p. 250505, 2007.
8. C.-Y. Lu, D. E. Browne, T. Yang, and J.-W. Pan, "Demonstration of a compiled version of shor's quantum factoring algorithm using photonic qubits," *Phys. Rev. Lett.* **99**(25), p. 250504, 2007.
9. S. Gaertner, M. Bourennane, C. Kurtsiefer, A. Cabello, and H. Weinfurter, "Experimental demonstration of a quantum protocol for byzantine agreement and liar detection," *Phys. Rev. Lett.* **100**(7), p. 070504, 2008.
10. C. Schmid, N. Kiesel, U. K. Weber, R. Ursin, A. Zeilinger, and H. Weinfurter, "Quantum teleportation and entanglement swapping with linear optics logic gates," *New J. Phys.* **11**(3), p. 033008 (10pp), 2009.
11. C.-Y. Lu, W.-B. Gao, O. Gühne, X.-Q. Zhou, Z.-B. Chen, and J.-W. Pan, "Demonstrating anyonic fractional statistics with a six-qubit quantum simulator," *Phys. Rev. Lett.* **102**(3), p. 030502, 2009.
12. J. K. Pachos, W. Wieczorek, C. Schmid, N. Kiesel, R. Pohlner, and H. Weinfurter, "Revealing anyonic features in a toric code quantum simulation," *New J. Phys.* **11**(8), p. 083010 (10pp), 2009. arXiv:0710.0895 [quant-ph].
13. D. Bouwmeester, J.-W. Pan, M. Daniell, H. Weinfurter, and A. Zeilinger, "Observation of three-photon greenberger-horne-zeilinger entanglement," *Phys. Rev. Lett.* **82**(7), pp. 1345–1349, 1999.
14. J.-W. Pan, M. Daniell, S. Gasparoni, G. Weihs, and A. Zeilinger, "Experimental Demonstration of Four-Photon Entanglement and High-Fidelity Teleportation," *Phys. Rev. Lett.* **86**(20), pp. 4435–4438, 2001.
15. M. Eibl, N. Kiesel, M. Bourennane, C. Kurtsiefer, and H. Weinfurter, "Experimental realization of a three-qubit entangled w state," *Phys. Rev. Lett.* **92**(7), p. 077901, 2004.
16. Z. Zhao, Y.-A. Chen, A.-N. Zhang, T. Yang, H. J. Briegel, and J.-W. Pan, "Experimental demonstration of five-photon entanglement and open-destination teleportation," *Nature* **430**(6995), pp. 54–58, 2004.
17. N. Kiesel, C. Schmid, U. Weber, G. Toth, O. Gühne, R. Ursin, and H. Weinfurter, "Experimental analysis of a four-qubit photon cluster state," *Phys. Rev. Lett.* **95**(21), p. 210502, 2005.
18. Q. Zhang, A. Goebel, C. Wagenknecht, Y.-A. Chen, B. Zhao, T. Yang, A. Mair, J. Schmiedmayer, and J.-W. Pan, "Experimental quantum teleportation of a two-qubit composite system," *Nat. Phys.* **2**, pp. 678–682, Oct. 2006.
19. N. Kiesel, C. Schmid, G. Tóth, E. Solano, and H. Weinfurter, "Experimental observation of four-photon entangled dicke state with high fidelity," *Phys. Rev. Lett.* **98**(6), p. 063604, 2007.
20. C.-Y. Lu, X.-Q. Zhou, O. Gühne, W.-B. Gao, J. Zhang, Z.-S. Yuan, A. Goebel, T. Yang, and J.-W. Pan, "Experimental entanglement of six photons in graph states," *Nat. Phys.* **3**, pp. 91 – 95, Feb. 2007.
21. W. Wieczorek, C. Schmid, N. Kiesel, R. Pohlner, O. Gühne, and H. Weinfurter, "Experimental observation of an entire family of four-photon entangled states," *Phys. Rev. Lett.* **101**(1), p. 010503, 2008.
22. M. Aspelmeyer and J. Eisert, "Quantum mechanics: Entangled families," *Nature* **455**, pp. 180–181, Sept. 2008.
23. M. Radmark, M. Żukowski, and M. Bourennane, "Experimental test of fidelity limits in six-photon interferometry and of rotational invariance properties of the photonic six-qubit entanglement singlet state," *Phys. Rev. Lett.* **103**(15), p. 150501, 2009.
24. W. Wieczorek, R. Krischek, N. Kiesel, P. Michelberger, G. Toth, and H. Weinfurter, "Experimental entanglement of a six-photon symmetric dicke state," *Phys. Rev. Lett.* **103**(2), p. 020504, 2009. arXiv: 0903.2213 [quant-ph].
25. R. Prevedel, G. Cronenberg, M. S. Tame, M. Paternostro, P. Walther, M. S. Kim, and A. Zeilinger, "Experimental realization of dicke states of up to six qubits for multiparty quantum networking," *Phys. Rev. Lett.* **103**(2), p. 020503, 2009. arXiv: 0903.2212 [quant-ph].
26. R. Krischek, W. Wieczorek, A. Ozawa, N. Kiesel, P. Michelberger, T. Udem, and H. Weinfurter, "Ultraviolet enhancement cavity for ultrafast nonlinear optics and high-rate multiphoton entanglement experiments," *Nat. Photon.* **4**, pp. 170–173, Mar. 2010.
27. G. Tóth, W. Wieczorek, R. Krischek, N. Kiesel, P. Michelberger, and H. Weinfurter, "Practical methods for witnessing genuine multi-qubit entanglement in the vicinity of symmetric states," *New J. Phys.* **11**(8), p. 083002 (18pp), 2009. arXiv: 0903.3910 [quant-ph].

28. W. Wieczorek, *Multi-Photon Entanglement: Experimental Observation, Characterization, and Application of up to Six-Photon Entangled States*. PhD thesis, Ludwig-Maximilians-Universität München, 2009.
29. L. Mandel and E. Wolf, *Optical Coherence and Quantum Optics*, Cambridge University Press, 1995.
30. D. M. Greenberger, M. A. Horne, and A. Zeilinger, "Going beyond bell's theorem," in *Bell's Theorem, Quantum theory and Conceptions of the Universe*, pp. 69–72, Kluwer Academic Publishers, 1989.
31. J. Kempe, D. Bacon, D. A. Lidar, and K. B. Whaley, "Theory of decoherence-free fault-tolerant universal quantum computation," *Phys. Rev. A* **63**(4), p. 042307, 2001.
32. M. Bourennane, M. Eibl, S. Gaertner, C. Kurtsiefer, A. Cabello, and H. Weinfurter, "Decoherence-free quantum information processing with four-photon entangled states," *Phys. Rev. Lett.* **92**(10), p. 107901, 2004.
33. R. H. Dicke, "Coherence in spontaneous radiation processes," *Phys. Rev.* **93**(1), pp. 99–110, 1954.
34. J. K. Stockton, J. M. Geremia, A. C. Doherty, and H. Mabuchi, "Characterizing the entanglement of symmetric many-particle spin-(1/2) systems," *Phys. Rev. A* **67**(2), p. 022112, 2003.
35. M. Eibl, S. Gaertner, M. Bourennane, C. Kurtsiefer, M. Żukowski, and H. Weinfurter, "Experimental observation of four-photon entanglement from parametric down-conversion," *Phys. Rev. Lett.* **90**(20), p. 200403, 2003.
36. N. Kiesel, *Experiments on Multiphoton Entanglement*. PhD thesis, Ludwig-Maximilians-Universität München, 2007.
37. W. Wieczorek, N. Kiesel, C. Schmid, and H. Weinfurter, "Multiqubit entanglement engineering via projective measurements," *Phys. Rev. A* **79**(2), p. 022311, 2009. arXiv:0901.4091 [quant-ph].
38. W. Laskowski, M. Wiesniak, M. Żukowski, M. Bourennane, and H. Weinfurter, "Interference contrast in multisource few-photon optics," *J. Phys. B* **42**(11), p. 114004 (12pp), 2009.
39. H. S. Eisenberg, G. Khoury, G. A. Durkin, C. Simon, and D. Bouwmeester, "Quantum Entanglement of a Large Number of Photons," *Phys. Rev. Lett.* **93**(19), p. 193901, 2004.
40. S. Naumov, A. Fernandez, R. Graf, P. Dombi, F. Krausz, and A. Apolonski, "Approaching the microjoule frontier with femtosecond laser oscillators," *New J. Phys.* **7**, p. 216, 2005.
41. T. Südmeyer, S. V. Marchese, S. Hashimoto, C. R. E. Baer, G. Gingras, B. Witzel, and U. Keller, "Femtosecond laser oscillators for high-field science," *Nat. Photon.* **2**, p. 599, 2008.
42. G. N. Gol'tsman, O. Okunev, G. Chulkova, A. Lipatov, A. Semenov, K. Smirnov, B. Voronov, A. Dzardanov, C. Williams, and R. Sobolewski, "Picosecond superconducting single-photon optical detector," *Appl. Phys. Lett.* **79**(6), pp. 705–707, 2001.
43. A. Verevkin, J. Zhang, R. Sobolewski, A. Lipatov, O. Okunev, G. Chulkova, A. Korneev, K. Smirnov, G. N. Gol'tsman, and A. Semenov, "Detection efficiency of large-active-area nbn single-photon superconducting detectors in the ultraviolet to near-infrared range," *Appl. Phys. Lett.* **80**(25), pp. 4687–4689, 2002.
44. R. H. Hadfield, "Single-photon detectors for optical quantum information applications," *Nat. Photon.* **3**, pp. 696–705, Dec. 2009.
45. V. P. Yanovsky and F. W. Wise, "Frequency doubling of 100-fs pulses with 50% efficiency by use of a resonant enhancement cavity," *Opt. Lett.* **19**(23), pp. 1952–1954, 1994.
46. C. Gohle, T. Udem, M. Herrmann, J. Rauschenberger, R. Holzwarth, H. A. Schuessler, F. Krausz, and T. W. Hänsch, "A frequency comb in the extreme ultraviolet," *Nature* **436**, pp. 234–237, July 2005.
47. J. R. Jones, K. D. Moll, M. J. Thorpe, and J. Ye, "Phase-coherent frequency combs in the vacuum ultraviolet via high-harmonic generation inside a femtosecond enhancement cavity," *Phys. Rev. Lett.* **94**, p. 193201, 2005.
48. A. Ozawa, J. Rauschenberger, C. Gohle, M. Herrmann, D. R. Walker, V. Pervak, A. Fernandez, R. Graf, A. Apolonski, R. Holzwarth, F. Krausz, T. W. Hänsch, and T. Udem, "High harmonic frequency combs for high resolution spectroscopy," *Phys. Rev. Lett.* **100**(25), p. 253901, 2008.
49. T. Udem, R. Holzwarth, and T. W. Häensch, "Optical frequency metrology," *Nature* **416**, p. 233, 2002.
50. R. Szipöcs, K. Ferencz, C. Spielmann, and F. Krausz, "Chirped multilayer coatings for broadband dispersion control in femtosecond lasers," *Opt. Lett.* **19**, p. 201, 1994.
51. J. Petersen and A. Luiten, "Short pulses in optical resonators," *Opt. Express* **11**(22), pp. 2975–2981, 2003.

52. C. Gohle, *A Coherent Frequency Comb in the Extreme Ultraviolet*. PhD thesis, Ludwig-Maximilians-Universität München, 2006.
53. T. W. Hänsch and B. Couillaud, "Laser frequency stabilization by polarization spectroscopy of a reflecting reference cavity," *Opt. Comm.* **35**, pp. 441–444, Dec. 1980.
54. J. M. Boon-Engering, W. E. van der Veer, E. A. J. M. Bente, and W. Hogervorst, "Stabilization of an optical cavity containing a birefringent element," *Opt. Comm.* **140**(4-6), pp. 285 – 288, 1997.
55. S. T. Cundiff and J. Ye, "Colloquium: Femtosecond optical frequency combs," *Rev. Mod. Phys.* **75**, pp. 325–342, Mar 2003.
56. W. Dür, G. Vidal, and J. I. Cirac, "Three qubits can be entangled in two inequivalent ways," *Phys. Rev. A* **62**(6), p. 062314, 2000.
57. F. Verstraete, J. Dehaene, B. DeMoor, and H. Verschelde, "Four qubits can be entangled in nine different ways," *Phys. Rev. A* **65**(5), p. 052112, 2002.
58. M. Bourennane, M. Eibl, S. Gaertner, N. Kiesel, C. Kurtsiefer, and H. Weinfurter, "Entanglement persistency of multiphoton entangled states," *Phys. Rev. Lett.* **96**(10), p. 100502, 2006.
59. M. Murao, D. Jonathan, M. B. Plenio, and V. Vedral, "Quantum telecloning and multiparticle entanglement," *Phys. Rev. A* **59**(1), pp. 156–161, 1999.
60. M. Hillery, V. Bužek, and A. Berthiaume, "Quantum secret sharing," *Phys. Rev. A* **59**(3), pp. 1829–1834, 1999.
61. V. Giovannetti, S. Lloyd, and L. Maccone, "Quantum-enhanced measurements: Beating the standard quantum limit," *Science* **306**(5700), pp. 1330–1336, 2004.
62. W. Wieczorek et al. *in preparation* , 2010.
63. T. Bastin, S. Krins, P. Mathonet, M. Godefroid, L. Lamata, and E. Solano, "Operational families of entanglement classes for symmetric n-qubit states," *Phys. Rev. Lett.* **103**(7), p. 070503, 2009.
64. N. Kiesel, W. Wieczorek, S. Krins, T. Bastin, H. Weinfurter, and E. Solano, "Operational multipartite entanglement classes for symmetric photonic qubit states," *Phys. Rev. A* , p. in press, 2010. arXiv:0911.5112v1 [quant-ph].
65. C. Kurtsiefer, M. Oberparleiter, and H. Weinfurter, "High-efficiency entangled photon pair collection in type-ii parametric fluorescence," *Phys. Rev. A* **64**(2), p. 023802, 2001.
66. P. G. Kwiat, K. Mattle, H. Weinfurter, A. Zeilinger, A. V. Sergienko, and Y. Shih, "New high-intensity source of polarization-entangled photon pairs," *Phys. Rev. Lett.* **75**, pp. 4337–4341, Dec. 1995.
67. J. G. Rarity, "Interference of single photons from separate sources," *Ann. N. Y.* **755**, pp. 624–631, 1995.
68. M. Żukowski, A. Zeilinger, and H. Weinfurter, "Entangling photons radiated by independent pulsed sources," *Ann. N. Y.* **755**, pp. 91–102, 1995.
69. G. Tóth, "Detection of multipartite entanglement in the vicinity of symmetric dicke states," *J. Opt. Soc. Am. B* **24**(2), p. 275, 2007.
70. S. Campbell, M. S. Tame, and M. Paternostro, "Characterizing multipartite symmetric dicke states under the effects of noise," *New J. Phys.* **11**(7), p. 073039 (22pp), 2009. arXiv: 0903.3939 [quant-ph].
71. R. Horodecki, P. Horodecki, M. Horodecki, and K. Horodecki, "Quantum entanglement," *Rev. Mod. Phys.* **81**(2), p. 865, 2009.
72. O. Gühne and G. Tóth, "Entanglement detection," *Phys. Rep.* **474**(1-6), pp. 1 – 75, 2009.
73. M. Bourennane, M. Eibl, C. Kurtsiefer, S. Gaertner, H. Weinfurter, O. Gühne, P. Hyllus, D. Bruß, M. Lewenstein, and A. Sanpera, "Experimental detection of multipartite entanglement using witness operators," *Phys. Rev. Lett.* **92**, pp. 087902–4, Feb. 2004.